THE JOURNAL OF PHYSICAL CHEMISTRY B

ARTICLE

pubs.acs.org/JPCB

Simulated Glass Transition of Poly(ethylene oxide) Bulk and Film: A Comparative Study

Chaofu Wu*

Department of Chemistry and Materials Science, Hunan University of Humanities, Science and Technology, Loudi 417000, the People's Republic of China

ABSTRACT: Stepwise cooling molecular dynamics (MD) simulations have been carried out on the bulk and film models for poly(ethylene oxide) (PEO) to understand glass transition of amorphous polymer films. Three types of properties —density, energy, and dynamics—are computed and plotted against the temperature for the two systems. It has been confirmed that all these properties can reveal glass transition in both PEO bulk and film systems. All the determined glass transition temperatures (T_g's) drop in the same order of magnitude to the experimental data available. Among various methods, the T_g's obtained from the density and energy data are close to each other if the same space regions are defined, which can suggest the same free volume theory, and dynamic T_g's obtained from mean-squared displacements (MSDs) are highest, which can suggest the kinetic theory for structural relaxation. Consistently, all these T_g's obtained using different methods show that the T_g's of PEO film are lower than those of PEO bulk. The free surface layers of polymer films dictate this offset.

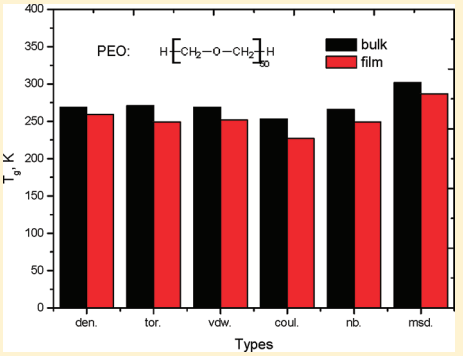

1. INTRODUCTION

Glass transition is one general phenomenon occurring in amorphous polymers. The temperature (T_g) characterizing it, around which many thermal and mechanical properties vary greatly, is well-known as one of most important parameters. In the literature, there are steady interests in understanding glass transition in various polymer systems. During the past decade, the hot points of such studies have shifted from bulks to confined films, which are widely used in a variety of technology fields, i.e., coatings, adhesives, and so forth.[1−4] Besides experimental methods for measuring T_g's, theoretical methods for predicting T_g's are quite desirable to practical applications. Recently, molecular simulations have become prevailing since they enable us to obtain sufficiently detailed information. On one hand, as pointed out by us,[5,6] glass transition of polymer bulks have been studied at the all-atomistic (AA) level using molecular simulations; on the other hand, glass transition of both free-standing and supported polymer films have mostly been studied with coarse-grained (CG) models.[7−13] Only very recently has the united-atom (UA) model came to be employed for studying glass transition of polymer films.[14−16] To our best knowledge, until now, only one article uses the AA model to simulate the glass transition of blend films of poly(phenylene oxide) (PPO)/polystyrene (PS) and poly(methyl methacrylate) (PMMA)/poly(ethylene oxide) (PEO).[17]

This trend of research identified above can be explained by the computational costs required, i.e. molecular simulations with CG models can study those phenomena covering much wider time and space scales than those based on AA models. However, it should be noted that the simulated T_g's based on CG models can not be directly compared to the corresponding experimental data, and thus, it is difficult to evaluate the effects of subtle structure on T_gs. Note that various atomistic molecular modeling methods have previously been developed and validated for representing polymer films.[18−26] With the great progress in computer techniques, now it is moderately feasible to study glass transition of polymer films using AA molecular simulations. It also has to be mentioned that most simulations of glass transition of polymer films are carried out on PS and other hydrocarbons. While early experiments focus on supported films, much of the recent research has targeted free-standing films.[3] Throughout these studies, emphasis was placed on how the T_g depends on the film thickness and interfacial interactions, and but only few studies were devoted to studying how the T_g's of polymer films differs from those of polymer bulks. Such an example includes the study in which Morita et al. performed a CG molecular simulation to understand glass transition in polymer films from the point of view of dynamics.[12]

In this work, fully atomistic molecular simulations have been extended to one typical nonhydrocarbon polymer, PEO, to more comprehensively understand the glass transition of polymer films. This synthetic polymer is investigated as one typical model because of its simple structure and versatile applications. The T_g's of PEO bulk and film systems are determined based on various properties—structure, energy, and dynamics. The main objective of this work is to make some quantitative comparisons between the two systems, and among various methods, and between the simulations and the experiments. In order to exclude the effects exerted by the substrates, an ultrathin free-standing polymer film is examined. Note that Baljon et al.[11] also carried out a similar study

Received: June 2, 2011
Revised: August 17, 2011
Published: August 22, 2011

dx.doi.org/10.1021/jp205205x | J. Phys. Chem. B 2011, 115, 11044–11052

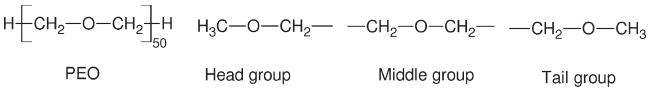

Figure 1. Chemical structure of PEO and its groups of atoms: head-group, middle group, and tail group.

to determine T_g using three different methods. The main difference from our work is that they employed a bead−spring model of supported polymer films, and computed different properties to determine T_g. Thus, the study presented here provides some new insights into the glass transition of polymer films.

2. COMPUTATIONAL DETAILS

The structural formula of a single PEO chain is displayed in Figure 1, together with the constituent residues. First, in Materials Studio-4.0 (Developed by Accelrys Co., http://www.accelrys.com/), one PEO chain was constructed from the residues using the "Visualizer" module and optimized using the "Discover" module. According to that reported by Luo and Jiang,[27] 50 monomers are sufficient to represent a PEO chain. Twenty optimized PEO chains were then packed into a three-dimensional (3D) periodic cubic box using the "Amorphous Cell" module. The initial cell dimension of box was defined by the arbitrary density of 1.0 g/cm^3 at 360 K. The as-obtained structure file (pdb format) was modified to be compatible with the academic package, GROMACS-4.5.3,[28,29] which was utilized thereafter for implementing all molecular simulations.

The energy of PEO bulk system was minimized alternately using the steep descent and conjugate gradient algorithms. This resulting model was subjected to two successive constant-NPT (constant number of atoms, pressure and temperature of system) molecular dynamics (MD) simulations at 360 K and 1 bar (1 bar = 10^5 Pa) for 10 and 5 ns, respectively. For the former, the Berendsen methods[30] were employed for controlling both temperature and pressure, whereas for the latter, the Nose−Hoover[31,32] and Parrinello−Rahman[33] methods were used for temperature and pressure coupling, respectively. The former aims to equilibrate the systems, whereas the latter aims to collect data. It should be noted that the coupling frequency was once every step, which is found important to obtain the proper densities. The stepwise cooling from 360 to 160 K was then applied to the as-obtained PEO bulk system, where constant-NPT MD was performed at every temperature. Along Mattice's method,[19,22,23,25] the free-standing PEO film system was prepared and centered by extending the C-dimension of the cubic box to 40 nm (1 nm = 10^{-9} m) without scaling the coordinates, where the C-dimension of box is parallel to the z-axis. The same stepwise cooling procedure was also applied to the PEO film system but with constant-NVT (constant number of atoms, volume and temperature of system) MD simulations. The MD simulation was run for 5 ns at every temperature, which was found adequate to equilibrate the systems for our purposes. That is, the system is regarded to be in equilibrium when the temperature, energy, root-mean-square deviation (rmsd) of atom distances, and/or density, become stable with simulation time. For the stepwise cooling procedures, the temperature interval was set as 20 K, so totally 11 temperatures were considered. The cooling rate can be roughly determined as 4×10^9 K/s, which is much higher than that in the experiments. We have also examined one smaller PEO system with 10 chains and obtained similar results.

The original OPLS-AA force field (FF) parameters,[34] together with the partial charges defined in COMPASS FF,[35] were employed for modeling the PEO systems. Although these treatments on charges are a bit arbitrary, the assigned values are close to the original ones defined in the OPLS-AA FF, and ensure that the whole systems are neutral in the charges. Moreover, such treatments on the partial charges have also been previously employed by us[6,36] and other authors,[37,38] which reasonably reproduce the experimental results. The van der Waals (vdw) interactions were computed utilizing a cutoff distance of 1.0 nm. To treat the Coulumbic interactions (coul.), the particle-mesh Ewald (PME) technique was employed. Long-range dispersion corrections were applied to both energy and pressure. None of bonds or angles was constrained during all the simulations. The initial velocities of atoms were generated at random according to a Maxwell distribution at the defined temperatures. A leapfrog algorithm was employed for integrating Newton's equations of motion, where the time step was set as 1 fs (1 fs = 10^{-15} s). The full MD trajectory was recorded every 1 ps for analyzing various properties of interest.

3. RESULTS

3.1. Density. According to the free volume theory, the thermal expansion coefficient of system would vary greatly when the system cools down from higher to lower temperature across the T_g. As in dilatometry experiments, the density is a quantity easy to measure in molecular simulations. Many simulation works demonstrated that, density or its reciprocal, specific volume, can be used to probe glass transition of polymer bulks.[6,15,27,39−42] Here, the densities of both systems are obtained by averaging over appropriate time and space windows. The last 4 ns of MD trajectories at each temperature is used, as the time domain otherwise specially declared. For the isotropic bulk system, the averaging of density is performed over the whole box. For the film system that is not isotropic, the averaging is performed over the center regions.

In Figure 2(a), the density profiles at various temperatures are depicted for the film system, which exhibit common characterizations of free-standing films: symmetry around the center (at z = 20 nm) and a sigmoid from the center to surface layer. Additionally, one higher temperature leads to less fluctuation in the density profiles, which agrees with the results reported by Baljon et al.[14] Note that 0.01 nm of slice distance has been set up for calculating these density profiles along the z-axis. Despite the fact that many authors have tried to use different definitions to determine the film thickness, the exact boundary between the center and surface layers is hard to define. However, the region with 18.5 nm < z < 21.5 nm can be surely classified into the center region, over which the averaged densities of film system is calculated. And the region with z < 18 nm or z > 22 nm surely belongs to the surface region. These boundary lines are all marked as dashes in Figure 2a.

In Figure 2b, the average densities described above are plotted as functions of temperature for the bulk and film systems, where the error bars are not displayed for clarity. The relative errors of these points in the figures, which are calculated as the results of standard deviations (sd's) divided by the averaging values, range from 2% to 14%, depending upon the temperature. We expect that one bigger model can reduce these relative errors because more samples are included. Notice that the density of bulk system at 300 K is about 1.100 g/cm^3, which compares well

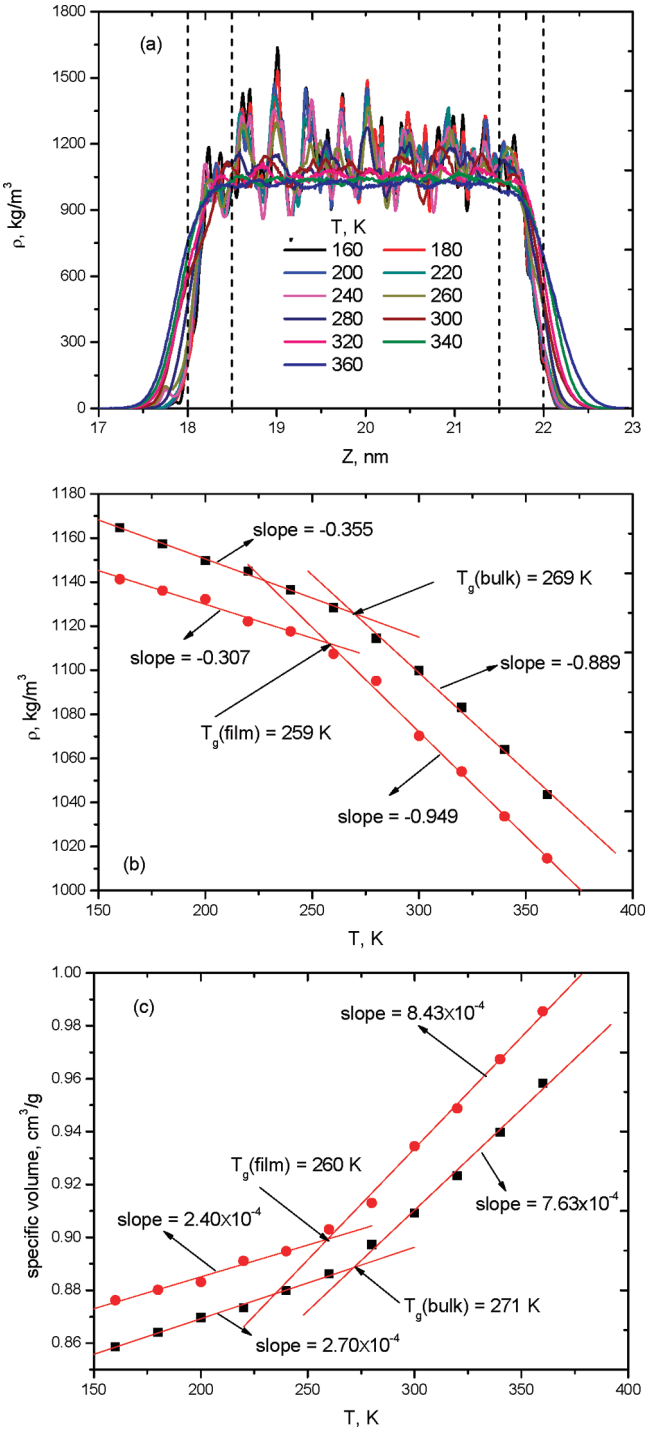

Figure 2. Density profiles of PEO film (a), and averaged densities (b) and specific volumes (c) of PEO bulk and the bulk region of film as functions of temperature.

with the corresponding experimental data 1.112[41] g/cm^3 or 1.07−1.27[27] g/cm^3. Additionally, at the same temperatures, the densities of the bulk system are higher than those of the film system. The densities of both systems increase with decreasing temperature. One obvious break can be observed in the plots, where two straight lines are used to fit the regions of lower (L-T) and higher temperatures (H-T). Also, the cross point of the two fitting lines is identified as the T_g. Therefore, the H-T regions correspond to the rubbery state, whereas the L-T regions correspond to the glassy state.

Table 1. Thermal Expansion Coefficient of PEO Bulk and Film at H-T and L-T Regions, Where They Are Calculated at T = 300 K (unit: $\times 10^{-4}$ K^{-1})

calculation type	temperature region	bulk	film
density	H-T	8.08	8.87
	L-T	3.22	2.86
specific volume	H-T	8.40	8.84
	L-T	2.94	2.57

Around the T_g's, the thermal expansion coefficient α changes abruptly, which is computed using[16]

$$\alpha = -\frac{1}{\rho}\left(\frac{d\rho}{dT}\right) \quad (1)$$

where ρ is the density of bulk or film system at temperature T. The simulated values of α for the bulk and film systems at T = 300 K are presented in Table 1. Obviously, for either the bulk or film system, the simulated α is higher for the melt state as compared to the glassy state. Also, at either the H-T region or the L-T region, the simulated thermal expansion coefficients are similar for the two systems. If the specific volumes are examined instead of the densities, similar results of α and T_g are obtained, as shown in Figure 2c and Table 1. The differences in α and T_g between those obtained using both methods can be traced to the departure of fitting points from the exact straight lines. Note that the obtained $\alpha = (8.08-8.40) \times 10^{-4}$ K^{-1} at the H-T region for the linear PEO bulk accords with the experimental result $\alpha = (6.53 \pm 0.14) \times 10^{-4}$ K^{-1} of Ribeiro and Freeman[43] for the cross-linked PEO bulk, which demonstrated that cross-links can lead to less volume expansions. This value is also in very good agreement with the $\alpha = 8.78 \times 10^{-4}$ K^{-1} at 298 K calculated by Bicerano's method[44] for the linear PEO with the same molecular weight (M_w).

3.2. Energy. Many experimental data demonstrate that glass transition must be companied by variation of energies.[1] Using simulations, Baljon et al.[11] calculated the temperature dependence of constant pressure heat capacities to determine T_g's. In molecular simulations, however, variations of potential energies can be measured more accurately than the heat capacities. Some characteristic breaks have been reported in the plots of internal energy,[39,45] intermolecular and intramolecular energies,[46] and torsion and nonbond energies[40−42] versus temperature. Thus, it can be a general characteristic of amorphous polymers that there exist some breaks in the plots of both torsion and nonbond energies versus temperature. Additionally, the temperatures where the breaks occur can be identified as T_g's.

Notice that such analyses on energy decomposition have been reported for polymer bulks but never for polymer films. To examine whether similar results also apply to polymer films, various energy components at those temperatures are calculated for both systems. For the OPLS-AA FF, the potential energy is sum of four components:

$$E = E_{bond} + E_{angle} + E_{tor} + E_{nb} \quad (2)$$

where the first three terms are bond E_{bond}, angle E_{angle} and torsion energies E_{tor}, respectively, and the last term named nonbond energy E_{nb} is the sum of van der Waals E_{vdw} and Coulombic interactions energies E_{coul}. The calculated results of E_{bond}, E_{angle}, E_{tor}, and E_{nb}, are depicted in figures 3(a)-3(c), respectively. The

dx.doi.org/10.1021/jp205205x |J. Phys. Chem. B 2011, 115, 11044–11052

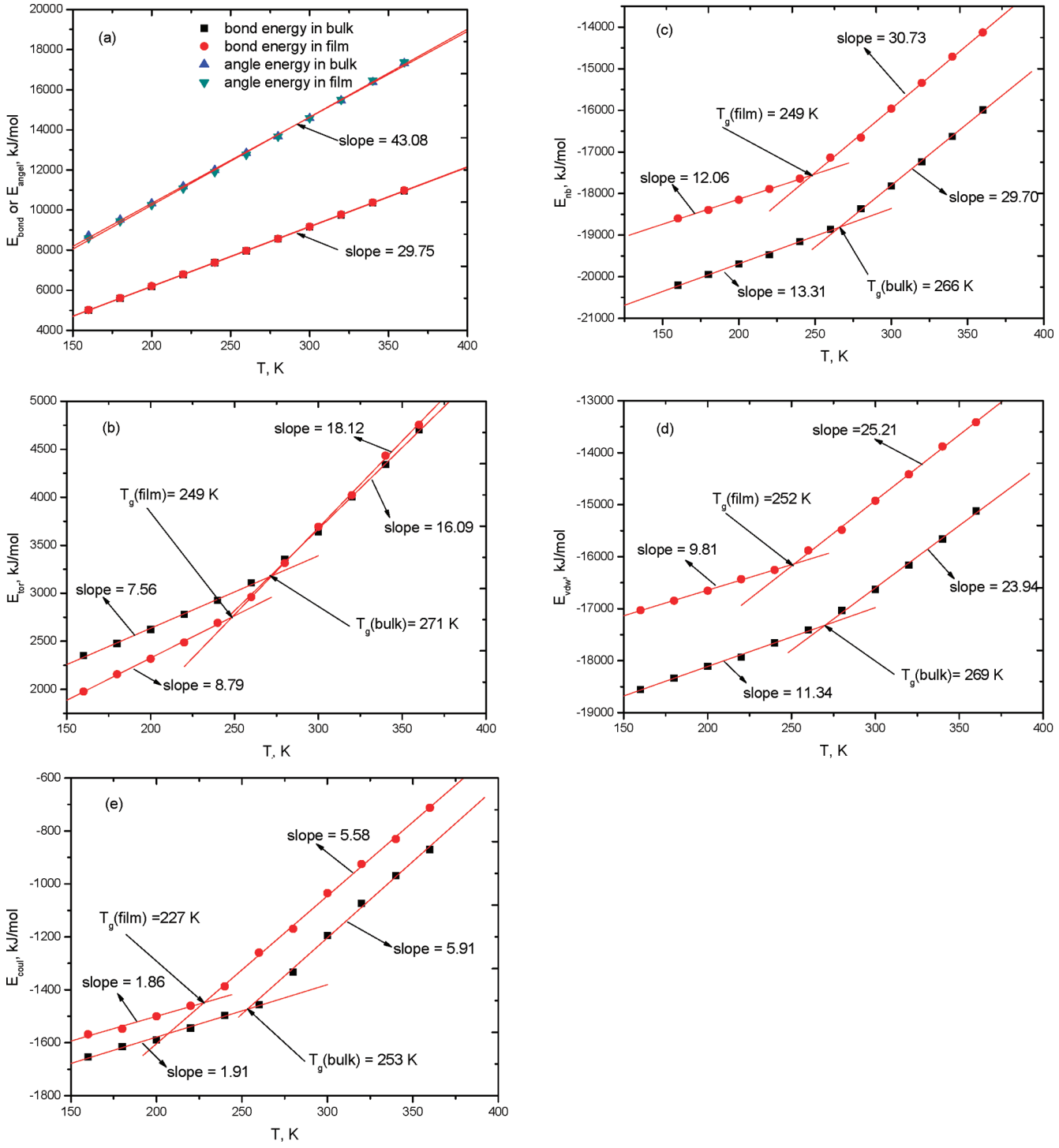

Figure 3. Various energy components versus temperature: bond energies E_{bond} and angle energies E_{angle} (a), torsion energies E_{tor} (b), nonbond energies E_{nb} (c), van der Waals interaction energies E_{vdw} (d), and Coulombic interaction energies E_{coul} (e).

relative errors of these points are all less than 1.4%, and the error bars are also not displayed in the figures for clarity.

It can be seen that, for the two systems, these energies increase with increasing the temperature. Specially, both bond and angle energies exhibit a good linearity with temperature over the whole range considered, which suggests that these degrees of freedom are in equilibrium.[42] For both systems, the bond energies at the same temperatures are higher than the angle energies, and the temperature has a little greater effect on the angle energies than bond energies. On the contrary, both torsion and nonbond energies show good linearity with temperature in the two temperature regions. Furthermore, van der Waals and Coulombic interaction energies are also plotted as functions of temperature in Figure 3d,e, indicating similar behaviors. It has to be mentioned that these E_{nb}, E_{vdw}, and E_{coul} are computed within the cutoff distance (i.e., short-range or SR). Nevertheless, when the long-

dx.doi.org/10.1021/jp205205x |J. Phys. Chem. B 2011, 115, 11044–11052

range (LR) corrections are considered in these energies, almost the same results are obtained. Note that Luo and Jiang carried out the same analyses on pure PEO bulk and its blends, only to demonstrate that the Coulombic energies did not exhibit pronounced kinks versus temperature.[27] This disageement can be explained by the FFs, i.e., the COMPASS[35] employed in their work uses cross items, whereas the OPLS-AA[34] employed in our work does not.

The glass transition temperatures, around which the energies present obvious breaks, are in practice identified as the temperatures corresponding to the cross points of two fitting lines. It has been confirmed that both torsion and nonbond energies play a crucial role in the glass transition of PEO bulk and film. The as-obtained T_g's for both bulk and film systems are also displayed in Figure 3. For both bulk and film systems, the T_g's obtained from Coulombic interaction energies are obviously lower than other T_g's, and all other T_g's are very similar to each other. Specially, T_g's obtained from E_{vdw}'s are closer to T_g's based on E_{nb}'s than those obtained from E_{coul}'s, suggesting that the van der Waals interactions are dominant in glass transition, which accords with the comments of Luo et al.[27] Furthermore, the change trends in energy components can be analyzed for both systems: (1) both bond and angle energies drop in the same lines, respectively; (2) the torsion energies drop in the same line in the H-T region but present two separated lines in the L-T region, where E_{tor}'s of the film system are higher than those of the bulk system; (3) the van der Waals, Coulombic, and total nonbond interactions energies exhibit two separated lines in both the H-T and L-T regions, where the corresponding energies of the film system are always higher than those of the bulk system.

3.3. Dynamics. At temperatures well above T_g, the molecules have a great deal of freedom to move, whereas at T_g or below, all these conformational changes of the backbone of the molecule are "frozen out".[47] Therefore, dynamic properties can also reveal evidence of the glass transition. In molecular simulations, dynamics of molecules can be conveniently characterized by means of the mean-squared displacement (MSD)

$$MSD(t) = \langle r^2(t)\rangle = \langle (1/N)\sum_{i=0}^{N}\sum_{X=x,y,z}|X_i(t) - X_i(0)|^2\rangle \quad (3)$$

In this formula, X_i is the x-, y- or z-coordinate of atom i, N is the total number of atoms, and the square bracket means averaging over the ensemble. Several groups have used MSD data to achieve T_g from MD simulations based on the mode coupling theory (MCT).[11] However, this method requires much more computational time beyond the capacity of current AA MD simulations, which are explained below. Alternatively, in another method developed by Tsige and Taylor[48] and by Bajon et al.,[14] the MSD within a short time interval is plotted as functions of temperature where the T_g is identified as the break temperature in the plot. In this section, this method is also employed to predict T_g's for the PEO bulk and film.

Figure 4a shows the MSD data of all atoms for PEO bulk in the entire time region (1−4000 ps) at various temperatures. It is seen that these MSD data almost have the scaling form

$$\log(\mathrm{MSD}) = a\cdot\log(t) + b \quad (4)$$

for the time region t = 10−100 ps, where a and b are constants. These fitting constants for various temperatures are presented in Table 2. According to the tube model,[12] one slope a = 0.5 corresponds to the unconstrained Rouse-like motion within a tube. For our case, the slopes at only the three higher temperatures studied are close to this condition. With the MCT,[11] the characteristic time τ of translational α-relaxation in the subdiffusive regime can be calculated using $\tau = 10^{-b/a}$, which is also presented in Table 2. It is found that the characteristic times at only two higher temperatures are not beyond the duration (5−10 ns) of our simulations, which restrict us to apply MCT or Vogel−Fulcher−Tammann (VFT) fitting to these data.

The MSD data at the shorter time interval t^* = 10 ps was used to characterize the temperature dependence of segment mobility. In Figure 4b, the MSD data at t^* = 10 ps are plotted against the temperatures for the PEO bulk and film. It can be seen that the MSDs for the two systems start to sharply increase at certain temperatures, which are identified as T_g's. The profiles of these MSD data are very similar to those reported by Morita et al.[12] in that there is one smooth transition between the H-T and L-T regions. The two straight lines are obtained by fitting data at the two ends representing H-T and L-T regions, respectively. According to Morita's comments,[12] the results of T_g's are independent of the choice of t^* if the scaling relation holds. However, one shorter time interval should be chosen for more samples included. We also use three different time intervals t^* = 1 ps, 100 ps, 1000 ps, only to find very similar results.

Notice that the MSD data presented above are calculated using all the 3D coordinates, which do not take into account the anisotropy of PEO film. To probe that, the MSDs have been separately computed along the three axes. One typical result of MSDs at 300 K is displayed in Figure 4c. It is seen that MSDs along the x- and y-axes (two dimensions (2D)) are similar to each other, especially for the time region $t \le$ 1500 ps, but quite different from those along the z-axis (one dimension (1D)). Therefore, two kinds of MSD data, one includes both x- and y-coordinates, whereas the other includes only z-coordinates, are calculated for the PEO film, which are denoted thereafter by MSD_{xy} and MSD_z, respectively. In Figure 4d,e, the MSD_z's and MSD_{xy}'s at t^* = 10 ps are plotted as functions of temperature, respectively. One break can also be seen in all the plots where the temperature of cross point fitting H-T and L-T regions is identified as T_g. It is found that the T_g's obtained from both 2D and 1D data are very close to that obtained from 3D data, indicating that the glass transition of polymer film is almost isotropy, as expected for amorphous polymers.

Furthermore, in order to assess the effects of free surface, the entire polymer film is divided into two layers along z-axis according to the density profile. Namely, an atom n is regarded to be in the center layer for the time interval t if the average z coordinate $[z_n(t') + z_n(t' + t)]/2$ is between 18.5 and 21.5 nm, otherwise it is regarded to be in the surface layer if the value is either less than 18 nm or more than 22 nm. The MSDs for the center layer and the surface layer are calculated separately according to Morita's definition:[12]

$$\phi_l(t) = \frac{\sum_{t'}\sum_{n\ \text{in layer}l}\sum_{X=x,y\ \text{or}\ z}[X_n(t'+t) - X_n(t')]^2}{\sum_{t'}\sum_{n\ \text{in layer}l}1} \quad (5)$$

With a small difference from Morita's definition,[12] only x- and y-dimensions (2D) or z-dimension (1D) data are included in the calculations. Note that this treatment of 2D data has also been employed for the entire film by Baljon et al.[11]

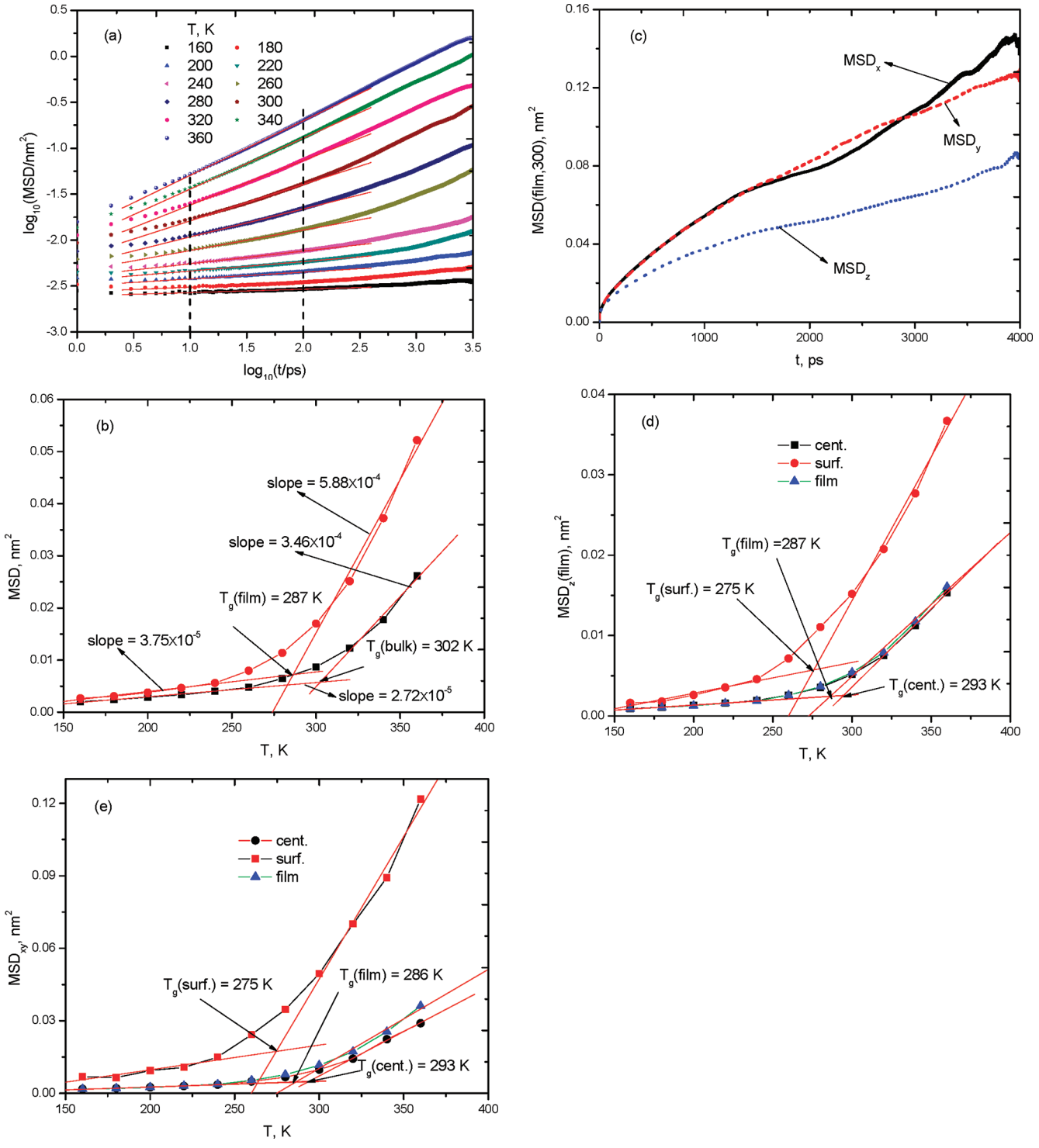

Figure 4. MSDs as functions of simulation time for the PEO bulk system (a), and MSDs at t^* = 10 ps versus temperature for the PEO bulk and film systems (b), and MSDs along the *x*-, *y*-, and *z*-axes as functions of simulation time for the PEO film system typically at 300 K (c), and MSD$_z$'s at t^* = 10 ps versus temperature (d), and MSD$_{xy}$'s at t^* = 10 ps versus temperature (e) for the center and surface layers of PEO film and the entire film.

In Figure 4d,e the MSD$_z$'s and MSD$_{xy}$'s at t^* = 10 ps versus temperature are also displayed for the center and surface layers of PEO film. It has been typically demonstrated that the segment mobility of the surface layer is much higher than that of the center layer, and the segment mobility of entire film is between those of the surface and center layers and is closer to that of the center layer. These results are in good agreements with the experimental data.[2] It can be obviously seen that one break occurs in both center and surface layers in the film. The break temperatures are identified as T_g's for the center and surface layers and entire film. The as-obtained T_g's take this order: T_g(center) > T_g(film) > T_g(surf), which accords with the delayed glassification (DG) model developed by Lipson and Milner.[3]

dx.doi.org/10.1021/jp205205x |*J. Phys. Chem. B* 2011, 115, 11044–11052

Table 2. Linear Fitting Constants of MSDs between 10 and 100 ps for PEO Bulk According to eq 4′[a]

temperature, K	intercept	slope	characteristic time, ps
360	−1.89	0.59	1597.3
340	−2.00	0.56	3727.6
320	−2.11	0.49	>20000
300	−2.19	0.40	>200000
280	−2.27	0.30	N/A
260	−2.34	0.22	N/A
240	−2.40	0.14	N/A
220	−2.44	0.10	N/A
200	−2.50	0.07	N/A
180	−2.56	0.05	N/A
160	−2.60	0.04	N/A

[a] All standard derivations are less than 0.003; N/A means enormously beyond our simulation duration (5−10 ns).

4. DISCUSSION

4.1. Validation of Methods for Predicting T_g's. It has been demonstrated that three types of properties—density, energy, and dynamics—can be used to reveal glass transition in both PEO bulk and film, and thus to predict T_g's of those systems. Note that these methods are all based on the fact that the calculated properties change almost linearly with increasing temperature within the two regions, and that the T_g's are identified as cross temperatures of two fitting lines to the H-T and L-T regions. As is pointed out, there is some degree of subjectivity in determining T_g's using this method, since it depends upon the temperature range chosen for representing the linear portions.[11] However, the identified linear portions in general exhibit higher correlation coefficients ($R \geq 0.99$ except the density data at L-T regions and the MSD data for which $R \geq 0.96$), which ensure us that these methods are not too arbitrary. The slopes of straight lines are displayed in figures to tell the difference. The simulated T_g's for the PEO bulk and film systems are summarized in table 3. In order to validate these simulation methods, it is instructive to make some elaborate comparisons among the T_g's.

4.2. Comparisons with the Experimental Data. Some conflicting experimental data have been reported in the literature for the PEO bulk system.[49] Depending upon the molecular weight (M_w), the experimental T_g's of a PEO bulk system can range from 190 to 256 K as well.[50,51] As is pointed out, this unusual behavior can be attributed to the change of crystallinity. For the two systems studied in this work, crystallization is not obviously observed from the plots of MSDs versus time, indicating that they are in essence amorphous. As is frequently commented out,[5,6] the quicker cooling rate in simulations than that in experiments can enhance the T_g's up to 20−30 K. Therefore, it can be concluded that our simulated values of T_g's are all in the same order of magnitude to the experimental data available. Note that Luo and Jiang obtained a simulated T_g value 251 K for the PEO bulk with the M_w = 3.96 kg/mol using the density data.[27] It can be seen that the T_g obtained by us with the same method is higher than this value by 18 K. Once again, this disagreement can be explained by the FF employed. However, the M_w is not expected to significantly affect the difference since the M_w of PEO studied in this work, ∼2.2 kg/mol, is very close to the experimental entanglement molecular weight M_e = 2.16 kg/mol.[50,52] For the PEO film, the comparisons become even more difficult since the film thickness and surface energy also significantly affects T_g.[1] No corresponding experimental T_g for PEO films can be found in the literature for comparison.

Table 3. Glass Transition Temperatures (T_g's) and the Deviation Obtained from Various Methods for the PEO Bulk and Film Systems (unit: K)

calculation type	T_g(bulk)	T_g(film)	$\Delta = T_g(\text{bulk}) - T_g(\text{film})$
density	269	259	+10
torsion energy	271	249	+22
vdw energy	269	252	+17
coul. energy	253	227	+26
nonbond energy	266	249	+17
MSDs	302	287	+15

4.3. Comparisons between Various Types of T_g's. For the PEO bulk system, the obtained T_g's from the density, torsion energy, and nonbond energy data are very close to each other, which can suggest that the same mechanism occurs in the glass transition, i.e., it is due to mainly the free volume theory. For the PEO film, however, the T_g obtained from density data is a bit higher than the those obtained from energy data. This can be reasonably explained as the former corresponding to the T_g of bulk region, whereas the latter corresponds to the T_g's of entire film. This concept is in good agreement with the fact that the T_g of the center layer based on MSDs is higher than that of the surface layer for the PEO film. The derived T_g's from MSDs for PEO bulk and film systems are obviously higher than those obtained from all other methods, which are in good agreement with the results (Figures 5 and 6 in ref 12) presented by Morita et al. for a PS bulk system, although they declared in the text that the T_g's based on MSDs compared well with those obtained from density data.[12] The results (Table 1 in ref 14) reported by Baljon et al.[14] also seem to support this statement. The glass transition as suggested by MSDs can be attributed to one different mechanism as suggested by density and energy, i.e., it can be due to mainly the kinetic theory for structural relaxation. Note that the concept of two distinct transitions has been put forward by Baljon et al.[11] to explain the simulated results. Additionally, in a series of papers, Freed and Douglas have also discussed this concept in depth.[53,54]

4.4. Comparisons between the Bulk and Film Systems. As showed by many experimental and simulation studies,[1,2,4,7−9,11,13,15] disparity in T_g's of polymer films from polymer bulks depends upon the interactions between polymers and substrates. Particularly, for ultrathin free-standing polymer films, the free surfaces always cause reduction in the T_g's of the entire films. It can be obviously seen from Table 3 that, for either method, the T_g's of PEO bulk are consistently higher than those of PEO film, which confirms these results. The distinction between the T_g's of two systems ranges from 10 to 26 K with different methods. The minimal distinction 10 K is due to density because this T_g corresponds to that of the center layer in the PEO film. This difference in T_g's derived from density data is very close to that (9 K) in dynamic T_g's obtained from MSD data if the same regions are considered. It is not surprising since the center layer in the film is slightly affected by the surface layers.[2] Also, the maximal distinction 26 K is due to T_g obtained from Coulombic energy, which suggests that Coulomb interactions among those energy components play the most important roles in the disparity of T_g's between the bulk and film systems. Other distinctions are medium and can be considered close to each other within the acceptable errors. Therefore, the reductions in T_g's of polymer films as compared to the polymer bulks can be attributed to the great

differences in structure and dynamics between the center layers and the free surfaces, which have been discussed above.

5. CONCLUSION

AA MD simulations have been extensively employed for studying glass transition in an ultrathin free-standing PEO film. As in the PEO bulk, the density of the center layer, the torsion and nonbond energies, and the MSDs can reveal glass transition in the PEO film, i.e., the plots of these properties versus temperature present some breaks. The T_g's are identified as the cross temperatures of two linear lines best-fitting to the H-T and L-T regions separated by some breaks. All the as-obtained T_g's drop in the same order of magnitude to the experimental data available. For the PEO bulk, the T_g's obtained from the densities and energies are similar to each other, while for the PEO film, there is a slight difference between the two types of T_g's because the density T_g's and energy T_g's correspond to the bulk layer and entire film, respectively. Furthermore, for both PEO bulk and film, van der Waals interactions are found to play a more important role in glass transition than Coulombic interactions. Thus, glass transition as revealed by densities and energies can suggest the same mechanism, i.e., free volume theory. Additionally, the T_g's obtained from MSDs are the highest among T_g's from various methods, which can show one different mechanism, i.e., kinetic theory of structural relaxation. The simulated results also show that, for all methods, the T_g's of PEO film are lower than those of PEO bulk. This can be due to more free volume and faster mobility of surface layers as compared to the bulk layers. In summary, this work provides some new insights into glass transition in polymer film. Moreover, this work demonstrates in some degree the validation of all three types of methods for predicting T_g's of polymer films, especially for quantifying the trends of T_g's, which can be widely used in the research and design (R&D) of related materials to polymer films. It should be mentioned that all these methods have different applications for predicting T_g's of polymer films: the density methods for center layers, the energy methods for entire film, and the dynamic methods for all makeup layers and entire films.

AUTHOR INFORMATION

Corresponding Author

*E-mail: xiaowu759@hotmail.com; xiaowu759@qq.com.

ACKNOWLEDGMENT

This work is supported by the start-up funds provided by the school to the author. The author is indebted to the Molecular Simulation Center of Hunan Province (situated Hunan University), which provides the commercial software (Materials Studio-4.0) to help build the PEO models, and the Laboratory for High Performance Computing (HPC) which provides the generous CPU times for completing this work. Two colleagues, Dr. Meixiu Wan and Mr. Xiuying Tian, are greatly appreciated for aiding in the revision of the manuscript.

REFERENCES

(1) Fryer, D. S.; Peters, R. D.; Kim, E. J.; Tomaszewski, J. E.; de_Pablo, J. J.; Nealey, P. F. Dependence of the Glass Transition Temperature of Polymer Films on Interfacial Energy and Thickness. *Macromolecules* **2001**, *34*, 5627–5634.

(2) Yang, Z.; Fujii, Y.; Lee, F. K.; Lam, C.-H.; Tsui, O. K. C. Glass Transition Dynamics and Surface Layer Mobility in Unentangled Polystyrene Films. *Science* **2010**, *328*, 1676–1679.

(3) Lipson, J. E. G.; Milner, S. T. Local and Average Glass Transitions in Polymer Thin Films. *Macromolecules* **2010**, *43*, 9874–9880.

(4) Sharp, J. S.; Forrest, J. A. Free Surfaces Cause Reductions in the GlassTransition Temperature of Thin Polystyrene Films. *Phys. Rev. Lett.* **2003**, *91*, 235701.

(5) Wu, C.; Xu, W. Atomistic Molecular Simulations of Structure and Dynamics of Crosslinked Epoxy Resin. *Polymer* **2007**, *48*, 5802–5812.

(6) Wu, C. Cooperative Behavior of Poly(vinyl alcohol) and Water As Revealed by Molecular Dynamics Simulations. *Polymer* **2010**, *51*, 4452–4460.

(7) Torres, J. A.; Nealey, P. F.; de Pablo, J. J. Molecular Simulation of Ultrathin Polymeric Films near the Glass Transition. *Phys. Rev. Lett.* **2000**, *85*, 3221–3224.

(8) Jain, T. S.; de Pablo, J. J. Monte Carlo Simulation of Free-Standing Polymer Films near the Glass Transition Temperature. *Macromolecules* **2002**, *35*, 2167–2176.

(9) Varnik, F.; Baschnagel, J.; Binder, K. Reduction of the Glass Transition Temperature in Polymer Films: A Molecular-Dynamics Study. *Phys. Rev. E* **2002**, *65*, 021507.

(10) Smith, G. D.; Bedrov, D.; Borodin, O. Structural Relaxation and Dynamic Heterogeneity in a Polymer Melt at Attractive Surfaces. *Phys. Rev. Lett.* **2003**, *90*, 226103.

(11) Baljon, A. R. C.; Weert, M. H. M.; DeGraaff, R. B.; Khare, R. Glass Transition Behavior of Polymer Films of Nanoscopic Dimensions. *Macromolecules* **2005**, *38*, 2391–2399.

(12) Morita, H.; Tanaka, K.; Kajiyama, T.; Nishi, T.; Doi, M. Study of the Glass Transition Temperature of Polymer Surface by Coarse-Grained Molecular Dynamics Simulation. *Macromolecules* **2006**, *39*, 6233–6237.

(13) Peter, S.; Meyer, H.; Baschnagel, J. Thickness-Dependent Reduction of the Glass-Transition Temperature in Thin Polymer Films with a Free Surface. *J. Polym. Sci., Part B: Polym. Phys.* **2006**, *44*, 2951–2967.

(14) Baljon, A. R. C.; Williams, S.; Balabaev, N. K.; PAANS, F.; Hudzinskyy, D.; Lyulin, A. V. Simulated Glass Transition in Free-Standing Thin Polystyrene Films. *J. Polym. Sci., Part B: Polym. Phys.* **2010**, *48*, 1160–1167.

(15) Yu, X.; Wu, R.; Yang, X. Molecular Dynamics Study on Glass Transitions in Atactic-Polypropylene Bulk and Freestanding Thin Films. *J. Phys. Chem. B* **2010**, *114*, 4955–4963.

(16) Hudzinskyy, D.; Lyulin, A. V.; Baljon, A. R. C.; Balabaev, N. K.; Michels, M. A. J. Effects of Strong Confinement on the Glass-Transition Temperature in Simulated Atactic Polystyrene Films. *Macromolecules* **2011**, *44*, 2299–2310.

(17) Ao, Z. M.; Jiang, Q. Size Effects on Miscibility and Glass Transition Temperature of Binary Polymer Blend Films. *Langmuir* **2006**, *22*, 1241–1246.

(18) Mansfield, K. F.; Theodorou, D. N. Atomistic Simulation of a Glassy Polymer Surface. *Macromolecules* **1990**, *23*, 4430–4445.

(19) Misra, S.; Fleming, P. D., III; Mattice, W. L. Structure and Energy of Thin Films of Poly-(1,4-c/s-butadiene): A New Atomistic Approach. *J. Comput.-Aided Mater. Des.* **1995**, *2*, 101–112.

(20) Aabloo, A.; Thomas, J. Molecular Dynamics Simulations of a Poly(ethylene oxide) Surface. *Comput. Theor. Polym. Sci.* **1997**, *7*, 47–51.

(21) Hapke, T.; Linke, A.; Patzold, G.; Heermann, D. W. Modeling of Amorphous Polymer Surfaces in Computer Simulation. *Surf. Sci.* **1997**, *373*, 109–124.

(22) Natarajan, U.; Tanaka, G.; Mattice, W. L. Atomistic Simulations of the Surfaces of Thin Films of Random Copolymers. *J. Comput.-Aided Mater. Des.* **1997**, *4*, 193–205.

(23) Natarajan, U.; Misra, S.; Mattice, W. L. Atomistic Simulation of a Polymer−Polymer Interface: Interfacial Energy and Work of Adhesion. *Comput. Theor. Polym. Sci.* **1998**, *8*, 323–329.

(24) Ito, M.; Matsumoto, M.; Doi, M. Molecular Dynamics Simulation of Polymer Film. *Fluid Phase Equilib.* **1998**, *144*, 395–401.

(25) Clancy, T. C.; Mattice, W. L. Computer Simulation of Polyolefin Interfaces. *Comput. Theor. Polym. Sci.* **1999**, *9*, 261–270.
(26) Ijantkar, A. S.; Natarajan, U. Atomistic Simulations of the Structure and Thermodynamic Properties of Poly(1,2-vinyl-butadiene) Surfaces. *Polymer* **2004**, *45*, 1373–1381.
(27) Luo, Z.; Jian, J. Molecular Dynamics and Dissipative Particle Dynamics Simulations for the Miscibility of Poly(ethylene oxide)/Poly(vinyl chloride) Blends. *Polymer* **2010**, *51*, 291–299.
(28) van_der_Spoel, D.; Lindahl, E.; Hess, B.; Groenhof, G.; Mark, A. E.; Berendsen, H. J. C. GROMACS: Fast, Flexible, and Free. *J. Comput. Chem.* **2005**, *26*, 1701–1718.
(29) Hess, B.; Kutzner, C.; van der Spoel, D.; Lindahl, E. GROMACS 4: Algorithms for Highly Efficient, Load-Balanced, and Scalable Molecular Simulation. *J. Chem. Theory. Comput.* **2008**, *4*, 435–447.
(30) Berendsen, H. J. C.; Postma, J. P. M.; van Gunsteren, W. F.; DiNola, A.; Haak, J. R. Molecular Dynamics with Coupling to an External Bath. *J. Chem. Phys.* **1984**, *81*, 3684–3690.
(31) Nose, S. A Molecular Dynamics Method for Simulations in the Canonical Ensemble. *Mol. Phys.* **1984**, *52*, 255–268.
(32) Hoover, W. G. Canonical Dynamics: Equilibrium Phase—Space Distributions. *Phys. Rev. A* **1985**, *31*, 1695–1697.
(33) Parrinello, M.; Rahman, A. Polymorphic Transitions in Single Crystals: A New Molecular Dynamics Method. *J. Appl. Phys.* **1981**, *52*, 7182–7190.
(34) Jorgensen, W. L.; Maxwell, D. S.; Tirado-Rives, J. Development and Testing of the OPLS All-Atom Force Field on Conformational Energetics and Properties of Organic Liquids. *J. Am. Chem. Soc.* **1996**, *118*, 11225–11236.
(35) Sun, H. COMPASS: An ab Initio Force-Field Optimized for Condensed-Phase Applications—Overview with Details on Alkane and Benzene Compounds. *J. Phys. Chem. B* **1998**, *102*, 7338–7364.
(36) Wu, C. pH Response of Conformation of Poly(propylene imine) Dendrimer in Water: A Molecular Simulation Study. *Mol. Simul.* **2010**, *36*, 1164–1172.
(37) Adisa, B.; Bruce, D. A. Molecular Dynamics Simulations of Helix-Forming, Amine-Functionalized *m*-Poly(phenyleneethynylene)s. *J. Phys. Chem. B* **2005**, *109*, 7548–7556.
(38) Adisa, B.; Bruce, D. A. Solvophobic and Steric Effects of Side Groups on Polymer Folding: Molecular Modeling Studies of Amine-Functionalized *m*-Poly(phenyleneethynylene) Foldamers in Aqueous Solution. *J. Phys. Chem. B* **2005**, *109*, 19952–19959.
(39) Fried, J. R.; Ren, P. Molecular Simulation of the Glass Transition of Polyphosphazenes. *Comput. Theor. Polym. Sci.* **1999**, *9*, 111–1116.
(40) Yu, K.-Q.; Li, Z.-S.; Sun, C.-C. Polymer Structures and Glass Transition: A Molecular Dynamics Simulation Study. *Macromol. Theory Simul.* **2001**, *10*, 624–633.
(41) Yang, H.; Li, Z.-S.; Qian, H.-J.; Yang, Y.-B.; Zhang, X.-B.; Sun, C.-C. Molecular Dynamics Simulation Studies of Binary Blend Miscibility of Poly(3-hydroxybutyrate) and Poly(ethylene oxide). *Polymer* **2004**, *45*, 453–457.
(42) Bermejo, J. S.; Ugarte, C. M. Influence of Cross-Linking Density on the Glass Transition and Structure of Chemically Cross-Linked PVA: A Molecular Dynamics Study. *Macromol. Theory Simul.* **2009**, *18*, 317–327.
(43) Ribeiro, C. P., Jr.; Freeman, B. D. Sorption, Dilation, and Partial Molar Volumes of Carbon Dioxide and Ethane in Cross-Linked Poly(ethylene oxide). *Macromolecules* **2008**, *41*, 9458–9468.
(44) Bicerano, J. *Prediction of Polymer Properties*, 3rd ed., revised and expanded; Marcel Dekker, Inc: New York, 2002.
(45) Rigby, D.; Roe, R.-J. Molecular Dynamics Simulation of Polymer Liquid and Glass. I. Glass Transition. *J. Chem. Phys.* **1987**, *87*, 7285.
(46) Soldera, A. Comparison Between the Glass Transition Temperatures of the Two PMMA Tacticities: A Molecular Dynamics Simulation Point of View. *Macromol. Symp.* **1998**, *133*, 21–32.
(47) Bower, D. I. *An Introduction to Polymer Physics*; Cambridge University Press: Cambridge, U.K., 2002.
(48) Tsige, M.; Taylor, P. L. Simulation Study of the Glass Transition Temperature in Polymethyl methacrylate. *Phys. Rev. E.* **2002**, *65*, 021805.
(49) Mark, J. E. *Polymer Data Handbook*; Oxford University Press, Inc.: Oxford, 1999.
(50) Niedzwiedz, K.; Wischnewski, A.; Pyckhout-Hintzen, W.; Allgaier, J.; Richter, D.; Faraone, A. Chain Dynamics and Viscoelastic Properties of Poly(ethylene oxide). *Macromolecules* **2008**, *41*, 4866–4872.
(51) Faucher, J. A.; Koleske, J. V.; Santee, E. R.; Stratta, J. J.; Wilson, C. W. Glass Transitions of Ethylene Oxide Polymers. *J. Appl. Phys.* **1966**, *37*, 3962–3964.
(52) Fetters, L. J.; Lohse, D. J.; Milner, S. T. Packing Length Influence in Linear Polymer Melts on the Entanglement, Critical, and Reptation Molecular Weights. *Macromolecules* **1999**, *32*, 6847–6851.
(53) Dudowicz, J.; Freed, K. F.; Douglas, J. F. Direct Computation of Characteristic Temperatures and Relaxation Times for Glass-Forming Polymer Liquids. *J. Chem. Phys.* **2005**, *123*, 111102.
(54) Dudowicz, J.; Freed, K. F.; Douglas, J. F. Fragility of Glass-Forming Polymer Liquids. *J. Phys. Chem. B* **2005**, *109*, 21350–21356.